



Photoluminescence of $\text{Lu}_3\text{Al}_5\text{O}_{12}:\text{Bi}$ and $\text{Y}_3\text{Al}_5\text{O}_{12}:\text{Bi}$ single crystalline films

V. Babin^a, V. Gorbenko^b, A. Krasnikov^a, A. Makhov^a, M. Nikl^c, S. Zazubovich^{a,*}, Yu. Zorenko^b

^a Institute of Physics, University of Tartu, Riia 142, 51014 Tartu, Estonia

^b Ivan Franko National University of Lviv, Gen. Tarnavsky 107, 79017 Lviv, Ukraine

^c Institute of Physics AS CR, Cukrovarnicka 10, 162 53 Prague, Czech Republic

ARTICLE INFO

Article history:

Received 3 August 2009

Received in revised form

2 September 2009

Accepted 7 December 2009

Keywords:

Bi^{3+} centers

Aluminium garnets

Photoluminescence

Localized excitons

ABSTRACT

Single crystalline films of $\text{Lu}_3\text{Al}_5\text{O}_{12}:\text{Bi}$ and $\text{Y}_3\text{Al}_5\text{O}_{12}:\text{Bi}$ have been studied at 4.2–450 K by the time-resolved luminescence spectroscopy method. Their emission spectrum consists of two types of bands with strongly different characteristics. The ultraviolet band consists of two components, arising from the electronic transitions which correspond to the $^3\text{P}_1 \rightarrow ^1\text{S}_0$ and $^3\text{P}_0 \rightarrow ^1\text{S}_0$ transitions in a free Bi^{3+} ion. At $T < 80$ K, mainly the lower-energy component with the decay time $\sim 10^{-3}$ s is observed, arising from the metastable $^3\text{P}_0$ level. At $T > 150$ K, the higher-energy component prevails, arising from the thermally populated emitting $^3\text{P}_1$ level. The visible emission spectrum consists of two dominant strongly overlapped broad bands with large Stokes shifts. At 4.2 K, their decay times are $\sim 10^{-5}$ s and $\sim 10^{-4}$ s and decrease with increasing temperature. Both of the visible emission bands are assumed to be of an exciton origin. The lower-energy band is ascribed to an exciton, localized near a single Bi^{3+} ion. The higher-energy band, showing a stronger intensity dependence on the Bi^{3+} content, is assumed to arise from an exciton, localized near a dimer Bi^{3+} center. The structure of the corresponding excited states is considered, and the processes, taking place in these states, are discussed.

© 2009 Elsevier Ltd. All rights reserved.

1. Introduction

Bi^{3+} -doped rare-earth aluminate and gallate garnets, where a Bi^{3+} ion substitutes a trivalent rare-earth ion, can be considered as prospective materials for scintillators due to an intense and fast Bi^{3+} -related emission (Nikl et al., 2005; Zorenko et al., 2007, 2009). However, the luminescence of Bi^{3+} centers in garnets has been studied in only a few papers. In the emission spectrum of $\text{Y}_3\text{Ga}_5\text{O}_{12}:\text{Bi}$ (Nikl et al., 2005; Setlur and Srivastava, 2006), $\text{Gd}_3\text{Ga}_5\text{O}_{12}:\text{Bi}$ (Setlur and Srivastava, 2006), $\text{Y}_3\text{Al}_5\text{O}_{12}:\text{Bi}$ (Setlur and Srivastava, 2006; Zorenko et al., 2007, 2009), and $\text{Lu}_3\text{Al}_5\text{O}_{12}:\text{Bi}$ (Setlur and Srivastava, 2006; Zorenko et al., 2009), two bands were observed, located in the ultraviolet and the visible spectral range. The ultraviolet emission was ascribed to the radiative decay of the triplet excited state of Bi^{3+} . Two components of this emission were ascribed to the electronic transitions, corresponding to the $^3\text{P}_1 \rightarrow ^1\text{S}_0$ and $^3\text{P}_0 \rightarrow ^1\text{S}_0$ transitions in a free Bi^{3+} ion (Nikl et al., 2005). The origin of the visible emission is still not clear. It was ascribed to the Bi^{3+} -related bound excitons (Ilmer et al., 1994) or to complex Bi^{3+} -based centers (Setlur and Srivastava, 2006; Zorenko et al., 2007, 2009). In single crystalline films of Bi^{3+} -doped aluminium garnets prepared

by the liquid phase epitaxy (LPE) method, a large and variable concentration of Bi^{3+} ions can be achieved (Zorenko et al., 2009).

The aim of the present work was to study the origin and structure of the excited states responsible for the luminescence of the $\text{Lu}_3\text{Al}_5\text{O}_{12}:\text{Bi}$ and $\text{Y}_3\text{Al}_5\text{O}_{12}:\text{Bi}$ single crystalline films and to clarify the processes taking place in their excited states.

2. Experimental

Single crystalline films (SCF) of $\text{Lu}_3\text{Al}_5\text{O}_{12}:\text{Bi}$ (LuAG:Bi) and $\text{Y}_3\text{Al}_5\text{O}_{12}:\text{Bi}$ (YAG:Bi) were grown by the LPE method from the melt-solution based on a Bi_2O_3 oxide flux (Zorenko et al., 2009). Three samples of LuAG:Bi with 0.07, 0.183 and 1.34 at% of Bi^{3+} and two samples of YAG:Bi with 0.133 and 0.92 at% of Bi^{3+} were studied.

The steady-state emission and excitation spectra were measured at 80–350 K under excitation in the 2.4–6.2 eV energy range at the set-up, consisting of a deuterium DDS-400 lamp, two monochromators and a photomultiplier with an amplifier and recorder. The spectra were corrected for the spectral distribution of the excitation light, the transmission and dispersion of the monochromators and the spectral sensitivity of the detectors. Luminescence decay kinetics in the microsecond to millisecond time range was measured at 4.2–300 K in the same set-up but under excitation with a xenon flash lamp FX-1152 (EG&G) (pulse duration of about

* Corresponding author. Tel.: +372 7 374 766; fax: +372 7 383 033.

E-mail address: svet@fi.tartu.ee (S. Zazubovich).

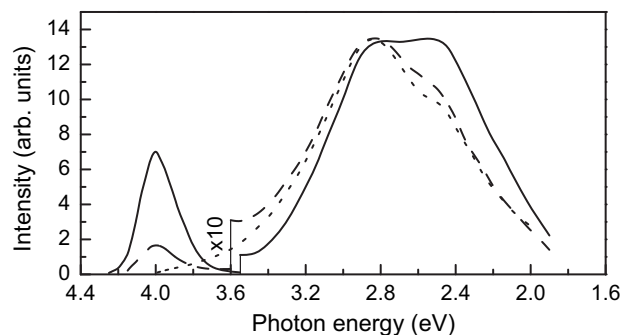


Fig. 1. Emission spectra (normalized) of YAG:Bi SCF measured at 80 K under 4.5 eV (solid line), 5.3 eV (dashed line) and 4.25 eV (dotted line) excitations. The intensity of the UV band is decreased 10 times. The spectra are distorted around 2.7 eV due to the contamination of the samples with Ce^{3+} ions and the reabsorption of the VIS emission in the ≈ 2.7 eV absorption band of Ce^{3+} centers.

1 μs and maximum repetition frequency of 300 Hz). The decay curves $I(t)$ were measured at the same conditions for different emission and excitation energies. This allows one to obtain the time-resolved emission and excitation spectra at any moment of time (t) after the excitation pulse. The $I(t)$ curves in the nanosecond time range were measured at 10–300 K under synchrotron excitation at SUPERLUMI station (HASYLAB at DESY, Hamburg, Germany). At 80–450 K, the decay kinetics were measured at a modified Spectrofluorometer 1995 (Edinburgh Instruments) under excitation with a nanosecond coaxial hydrogen-filled flashlamp (IBH Scotland) and using two single grating monochromators. The detection was performed using an IBH-04 photomultiplier module using the method of time-correlated single photon counting. A deconvolution procedure (SpectraSolve software package) was applied to extract true decay times using the multiexponential approximation. The experiments at low temperatures were carried out with the use of an immersion helium cryostat or vacuum nitrogen cryostat.

3. Results and discussion

The emission spectra of LuAG:Bi and YAG:Bi consist of two types of bands, located in the ultraviolet (UV) and the visible (VIS) spectral range (see, e.g., Fig. 1) and having strongly different characteristics. Both the UV and VIS bands are of a complex structure. The characteristics of their separate components are similar in LuAG:Bi and YAG:Bi (Table 1) and independent of the Bi^{3+} content. For LuAG:Bi, their detailed study has been recently carried out by us (Babin et al., 2009). Therefore, the luminescence characteristics of YAG:Bi are mainly reported in the present paper.

Table 1

The maxima positions (E_{max}) and halfwidths (FWHM) of the emission bands, the excitation bands maxima (E_{exc}), the Stokes shifts (S), and the luminescence decay times (τ) obtained for the UV and the VIS emission of Bi^{3+} -related centers in LuAG:Bi and YAG:Bi.

Sample	T (K)	E_{em} (eV)	FWHM (eV)	E_{exc} (eV)	S (eV)	τ at 4.2 K
LuAG:Bi	80	4.08	0.24	5.95; 4.63	0.55	1100 μs
	150	4.19	0.27	5.97; 4.63	0.44	0.1–0.4 ns
	80	2.60	0.87	5.95; 4.60	2.00	26 μs ; 72 μs
	80	2.75	0.90	5.20; 4.35	1.60	40 μs
YAG:Bi	80	3.99	0.24	5.90; 4.57	0.58	1050 μs
	150	4.11	0.27	5.90; 4.57	0.46	0.2–0.6 ns
	80	2.63	0.85	5.90; 4.55	1.92	38 μs ; 120 μs
	80	2.75	0.85	5.40; 4.32	1.57	33 μs

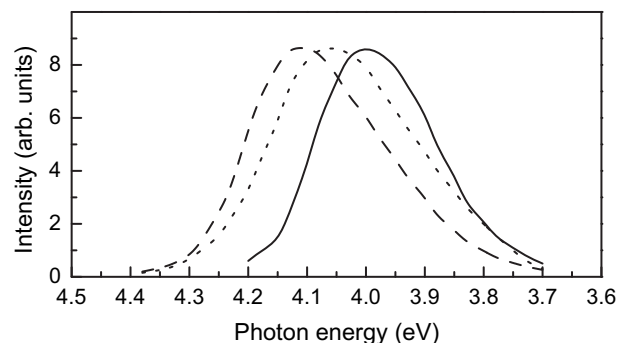


Fig. 2. Ultraviolet emission spectra (normalized) of YAG:Bi SCF measured at 80 K (solid line), 150 K (dashed line) and 300 K (dotted line). $E_{\text{exc}} = 4.5$ eV

3.1. Ultraviolet luminescence

At 80 K, the UV emission band of YAG:Bi is located at 3.99 eV (Fig. 2, solid line). In the excitation spectrum of this emission, wide bands around 5.9 eV and 4.57 eV are observed (Fig. 3, solid line). Their shape is distorted due to a very large optical density ($D > 3$). The UV band is shifting with increasing temperature (Fig. 4a, points) up to 4.11 eV at 150 K (Fig. 2, dashed line). These data indicate the presence of two components in the UV emission spectrum. The thermally stimulated redistribution of their intensities takes place around 110 K (Fig. 4a) with an activation energy $E_a \sim 100$ meV. As the temperature increases further, the emission band maximum is shifting back (Fig. 4a), down to 4.06 eV at 300 K (Fig. 2, dotted line). This shift is accompanied by the reverse redistribution of the emission intensities at $T > 170$ K (Fig. 4a). In the 4.2–140 K range, the maximum intensity of the UV emission decreases and then remains constant up to 330 K (Fig. 4b, solid line). In the decay kinetics of the UV emission, mainly a slow component is observed. At $T < 80$ K, its decay time is 1.05 ms. At $T > 125$ K, the decay time decreases with increasing temperature (Fig. 5a) with $E_a \sim 100$ meV. The time-resolved emission spectrum of this component is independent of t and is shown in the inset. At 4.2 K, a very weak fast component is also observed with decay time of 0.2–0.6 ns. Its lightsum is at least two orders of magnitude smaller compared with the lightsum of the slow component.

Comparison of the data obtained for YAG:Bi in the present paper and for LuAG:Bi by Babin et al. (2009) with those reported for the UV emission of Bi^{3+} centers in other hosts (see, e.g., Wolfert and Blasse, 1985; Donker et al., 1989; Aceves et al., 1996; Nikl et al., 2005) allows us to conclude that the 5.9 eV and 4.57 eV excitation bands arise from the electronic transitions to the singlet and

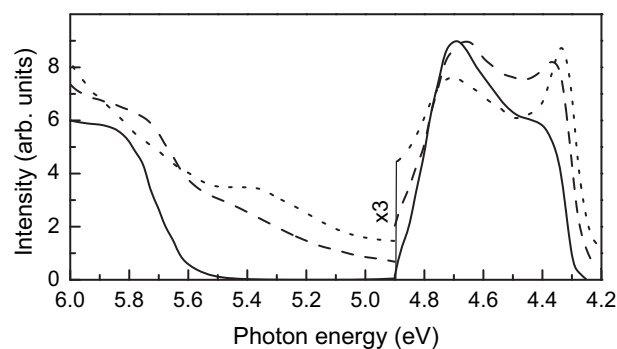


Fig. 3. Excitation spectra (normalized) of the UV emission (solid line) and of the VIS emission of YAG:Bi SCF measured for $E_{\text{em}} = 2.2$ eV (dashed line) and $E_{\text{em}} = 3.2$ eV (dotted line). $T = 80$ K.

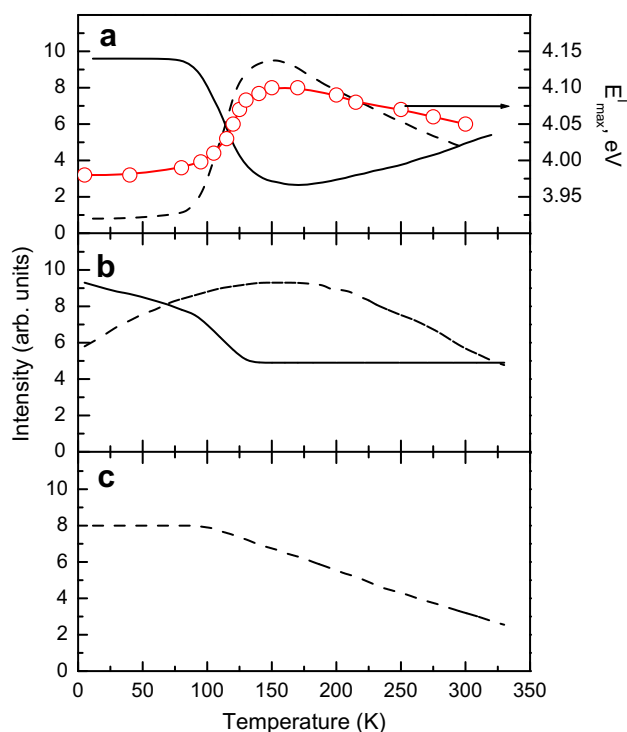


Fig. 4. Temperature dependences of (a) the maximum position of the UV emission band in YAG:Bi SCF (points) and the emission intensities (normalized) at $E_{em} = 3.8$ eV (solid line) and $E_{em} = 4.235$ eV (dashed line) measured under $E_{exc} = 4.5$ eV; (b) the maximum intensity of the UV emission (solid line) and the emission intensity at $E_{em} = 2.5$ eV (dashed line), both under $E_{exc} = 4.5$ eV; (c) the emission intensity at $E_{em} = 2.75$ eV under $E_{exc} = 5.3$ eV.

triplet excited states of Bi^{3+} centers, respectively, corresponding to the $^1S_0 \rightarrow ^1P_1$ and $^1S_0 \rightarrow ^3P_1$ transitions in a free Bi^{3+} ion. The two components of the UV emission can be ascribed to the electronic transitions, corresponding to the $^3P_1 \rightarrow ^1S_0$ and $^3P_0 \rightarrow ^1S_0$ transitions in a free Bi^{3+} ion. At low temperatures, the slow lower-energy component, arising from the metastable 3P_0 level, considerably prevails. At $T > 150$ K, the higher-energy component prevails, arising mainly from the thermally populated emitting 3P_1 level. The energy distance between these levels is about 100 meV. A strong shortening of the fast component decay time (by two orders of magnitude compared with that expected for the 3P_1 state of a Bi^{3+} -type center) can be caused by the fast non-radiative $^3P_1 \rightarrow ^3P_0$ transitions. A very small lightsum of this component may also mean that the initial population of the relaxed 3P_1 -related state is comparatively small and that the metastable 3P_0 -related minimum is mainly populated from the non-relaxed 3P_1 state.

3.2. Visible luminescence

The main excitation bands of the VIS emission in YAG:Bi are located around 5.9 eV, 5.4 eV, and 4.55 eV (Fig. 3, dashed and dotted lines). Under excitation around 4.55 eV and 5.9 eV, the emission band is peaking at 2.63 eV (Fig. 1, solid line). Under excitation at 5.3 eV (dashed line) and 4.25 eV (dotted line), the emission band maximum is located at 2.75 eV. The excitation spectra, measured for two opposite sides of the VIS band (at 2.2 eV and 3.2 eV), are different (Fig. 3). Temperature dependences of the emission intensities, measured under excitation in the 4.55 eV and 5.4 eV bands, are also different (compare dashed lines in Fig. 4b and c).

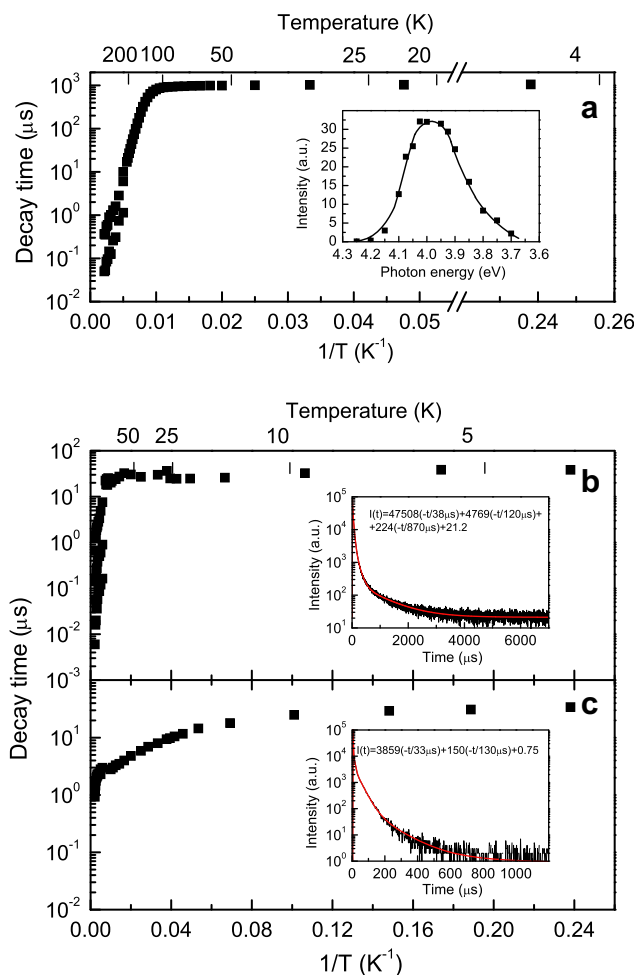


Fig. 5. (a) Temperature dependence of the UV emission decay time in YAG:Bi SCF measured at $E_{em} = 4.0$ eV under $E_{exc} = 4.55$ eV. The uncorrected time-resolved emission spectrum measured at 4.2 K at $t = 1000$ μs (the inset). (b,c) Temperature dependences of the visible emission decay times measured for (b) $E_{em} = 2.4$ eV, $E_{exc} = 4.5$ eV and (c) $E_{em} = 3.1$ eV, $E_{exc} = 5.2$ eV. The corresponding decay curves obtained at 4.2 K are shown in the insets.

Thus, the VIS emission band consists of at least two components. Their halfwidths (FWHM) and Stokes shifts are about three times larger compared with the UV bands (Table 1). In the 4.4–4.9 eV energy range, the excitation band of the 2.63 eV emission (Fig. 3, dashed line) is close to that of the UV emission (solid line). This can indicate that both these bands arise from the same Bi^{3+} center. This assumption is confirmed by the fact that the decrease of the UV emission intensity at 4.2–140 K (Fig. 4b, solid line) is accompanied by the increase of the 2.63 eV emission intensity (dashed line). The activation energy of both these processes is about 6–9 meV. As no shortening of the UV emission decay time is observed up to 100 K, these data indicate the presence of thermally stimulated transitions between the non-relaxed excited state, responsible for the UV emission, and the excited state, responsible for the 2.63 eV emission.

The decay kinetics of the VIS emission is very complicated. At 4.2 K under 4.5 eV excitation, the decay time of the strongest component is about 38 μs (Fig. 5b). As the temperature increases, it decreases with an activation energy of about 0.15 meV up to 50 K and with an activation energy of about 40 meV, at $T > 170$ K. The latter process is due to the thermal quenching of this emission (Fig. 4b, dashed line). The emission spectra of different decay components are close and located around 2.8 eV (FWHM ≈ 0.8 eV).

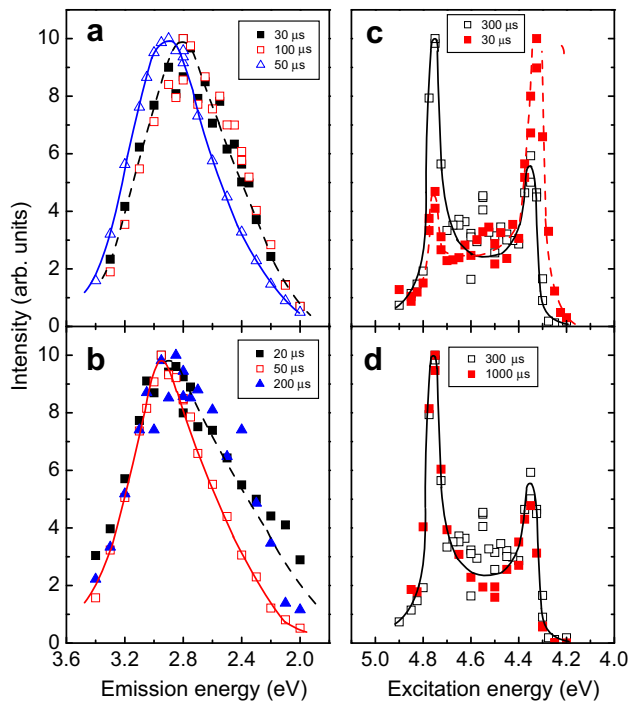


Fig. 6. Uncorrected time-resolved emission (a,b) and excitation (c,d) spectra of YAG:Bi SCF at 4.2 K. The emission spectra are measured: (a) at $t = 30 \mu\text{s}$ and $t = 100 \mu\text{s}$ under $E_{\text{exc}} = 4.5 \text{ eV}$ (dashed line) and at $t = 50 \mu\text{s}$ under $E_{\text{exc}} = 4.25 \text{ eV}$ (solid line); (b) at $t = 50 \mu\text{s}$ (solid line) and at $t = 200 \mu\text{s}$ and $t = 20 \mu\text{s}$ (dashed line) under $E_{\text{exc}} = 5.2 \text{ eV}$. The excitation spectra are measured: (c) for $E_{\text{em}} = 2.3 \text{ eV}$ at $t = 300 \mu\text{s}$ (solid line) and for $E_{\text{em}} = 3.1 \text{ eV}$ at $t = 30 \mu\text{s}$ (dashed line); (d) for $E_{\text{em}} = 2.3 \text{ eV}$ at $t = 300 \mu\text{s}$ and for $E_{\text{em}} = 4.0 \text{ eV}$ at $t = 1000 \mu\text{s}$ (solid line).

(Fig. 6a, dashed line). Under 5.3 eV excitation, two components are observed at 4.2 K with decay times of about 33 μs and 130 μs (Fig. 5c). The latter component is very weak. Probably this is the superposition of the slower ($\sim 120 \mu\text{s}$ and $\sim 870 \mu\text{s}$) components observed under 4.5 eV excitation. The value and temperature dependence of the decay time of the dominating 33 μs component is similar to that of the 38 μs component observed under 4.5 eV excitation (Fig. 5b). As the temperature increases, the decay time decreases with an activation energy of about 0.2 meV in the 4.2–10 K range and of about 4 meV, in the 25–100 K range. However, the time-resolved emission spectrum of this component (obtained at $t = 50 \mu\text{s}$, see Fig. 6b, solid line) is shifted to higher energies (up to 2.92 eV) and it is narrower (FWHM = 0.68 eV) than the spectra of the decay components observed under 4.5 eV excitation (Fig. 6a, dashed line). Thus, one can conclude that the 33 μs component arises from the higher-energy emission band and the 38 μs component from the lower-energy band. The 33 μs component is excited around 4.25 eV as well. This reveals itself in the high-energy shift (up to 2.9 eV) and narrowing (FWHM = 0.7 eV) of the time-resolved emission spectrum measured under this excitation at $t = 50 \mu\text{s}$ (Fig. 6a, solid line). The emission spectrum of the weak 130 μs component and the emission spectrum obtained at $t = 20 \mu\text{s}$ (Fig. 6b, dashed line) are close to the spectra obtained under 4.5 eV excitation (Fig. 6a, dashed line). It means that the decay components, characteristic for the lower-energy emission, appear under 5.3 eV excitation as well.

The time-resolved excitation spectra measured for the lower-energy (Fig. 6c, solid line) and the higher-energy (dashed line) components of the VIS emission are different. The 33 μs component, dominating in the decay kinetics of the higher-energy emission, is relatively more effectively excited at the low-energy edge of the 4.55 eV absorption band. The excitation spectra of the 38 μs

component and of the slower components, arising from the 2.63 eV emission, are close to the excitation spectrum of the UV emission (Fig. 6d).

The characteristics of the two visible emissions (the large Stokes shifts and FWHM, relatively small values of the slow component decay times at 4.2 K ($\sim 10^{-4}$ – 10^{-5} s) and their temperature dependences (e.g., the increase of the decay times with the decreasing temperature at $T < 4.2 \text{ K}$) are strongly different from the characteristics of the triplet UV emission of Bi^{3+} centers. However, they are similar to the characteristics of the visible emission of CsI:TI which has been ascribed by some of us to the exciton localized near a Ti^{4+} ion (Nagirnyi et al., 1994, 1995). This fact allows us to conclude that the both VIS emission bands of the Bi^{3+} -doped aluminium garnets are of an exciton origin. From the temperature dependences of their decay times one can estimate the energy distance between the emitting and the metastable minimum of the triplet exciton state ($\sim 0.1 \text{ meV}$) and the energy distance between the exciton triplet and singlet states ($\sim 1 \text{ meV}$). As the excitation spectra of the 2.63 eV emission and the UV emission are close and thermally stimulated transitions are detected between the corresponding excited states, both these emissions are assumed to arise from the same Bi^{3+} center. The 2.63 eV emission can be ascribed to an exciton localized near a single Bi^{3+} ion. The 2.75 eV emission shows a stronger intensity dependence on the Bi^{3+} content (Zorlenko et al., 2009). One can assume that it arises from an exciton localized near a dimer Bi^{3+} center. The charge-transfer processes, resulting in the formation of the localized exciton states under excitation in the Bi^{3+} -related absorption bands, can be similar to those proposed for CsI:TI (Babin et al., 2002). They are considered in more detail for LuAG:Bi (Babin et al., 2009).

4. Conclusions

The results obtained in the study of LuAG:Bi (Babin et al., 2009) and YAG:Bi (this paper) allow us to conclude that the Bi^{3+} -ion-related energy levels and the levels of an exciton, localized near the Bi^{3+} ion, coexist in the triplet relaxed excited state of the luminescence center. The radiative decay of the emitting and metastable minima, arising from the $^3\text{P}_1$ - and $^3\text{P}_0$ -related levels of a free Bi^{3+} ion, results in the appearance of two components of the UV emission. The radiative decay of the localized exciton results in the appearance of the lower-energy VIS emission band. Thermally stimulated transitions between the metastable and emitting minima of the triplet state of both the Bi^{3+} ion and the exciton localized near the Bi^{3+} ion, between the states of the Bi^{3+} ion and the localized exciton, and between the triplet and singlet states of the localized exciton reveal themselves in the low-temperature luminescence decay kinetics. The features observed in the photoluminescence of the Bi^{3+} -doped aluminium garnets and the peculiarities of their relaxed excited state structure are similar to those observed earlier by some of us for CsI:TI crystals.

The weak higher-energy VIS emission band, showing a stronger intensity dependence on the Bi^{3+} content, is assumed to arise from an exciton localized near a dimer Bi^{3+} center.

A similar excited state structure can be characteristic for Bi^{3+} -related centers also in some other Bi^{3+} -doped rare-earth garnets and perovskites.

Acknowledgements

This work was partly supported by the Estonian Science Foundation project No. 7507, the project of Czech Science Foundation No. 202/08/0893, the project of the Ukrainian Ministry of Education and Science No. SF-77 F, and the EC Research Infrastructure Action under the FP6 “Structuring the European Research Area”

Programme (“Integrating Activity on Synchrotron and Free Electron Laser Science”).

References

- Aceves, R., Barboza Flores, M., Maaros, A., Nagirnyi, V., Perez Salas, R., Tsuboi, T., Zazubovich, S., Zepelin, V., 1996. RES structure of Bi^{3+} centers in $\text{KCl}:\text{Bi}$ and $\text{CaO}:\text{Bi}$ crystals. *Phys. Status Solidi B* 194, 619–631.
- Babin, V., Kalder, K., Krasnikov, A., Zazubovich, S., 2002. Luminescence and defects creation under photoexcitation of $\text{CsI}:\text{Tl}$ crystal in Tl^+ -related absorption bands. *J. Lumin* 96, 75–85.
- Babin, V., Gorbenko, V., Krasnikov, A., Makhov, A., Nikl, M., Polak, K., Zazubovich, S., Zorenko, Yu., 2009. Peculiarities of excited state structure and photoluminescence in Bi^{3+} -doped $\text{Lu}_3\text{Al}_5\text{O}_{12}$ single crystalline films. *J. Phys. Condens. Matter* 21, 415502–415510 (9 pp).
- Donker, H., Yamashita, N., Smit, W.M.A., Blasse, G., 1989. Luminescence decay times of the Sb^{3+} , Pb^{2+} and Bi^{3+} ions in alkaline-earth sulfides. *Phys. Status Solidi B* 156, 537–544.
- Ilmer, M., Grabmaier, B.C., Blasse, G., 1994. Luminescence of Bi^{3+} in gallate garnets. *Chem. Mater* 6, 204–206.
- Nagirnyi, V., Zazubovich, S., Zepelin, V., Nikl, M., Pazzi, G.P., 1994. A new model for the visible emission of $\text{CsI}:\text{Tl}$ crystal. *Chem. Phys. Lett.* 227, 533–538.
- Nagirnyi, V., Stolovich, A., Zazubovich, S., Zepelin, V., Mihokova, E., Nikl, M., Pazzi, G.P., Salvini, L., 1995. Peculiarities of triplet relaxed excited state structure and luminescence of $\text{CsI}:\text{Tl}$ crystal. *J. Phys. Condens. Matter* 7, 3637–3653.
- Nikl, M., Novoselov, A., Mihokova, E., Polak, K., Dusek, M., McClune, B., Yoshikawa, A., Fukuda, T., 2005. Photoluminescence of Bi^{3+} in $\text{Y}_3\text{Ga}_5\text{O}_{12}$ single-crystal host. *J. Phys. Condens. Matter* 17, 3367–3375.
- Setlur, A.A., Srivastava, A.M., 2006. The nature of Bi^{3+} luminescence in garnet hosts. *Opt. Mater* 29, 410–415.
- Wolfert, A., Blasse, G., 1985. Luminescence of Bi^{3+} -activated LaOBr , a system with emission from different states. *J. Lumin.* 33, 213–226.
- Zorenko, Yu., Gorbenko, V., Voznyak, T., Vistovsky, V., Nedilko, S., Nikl, M., 2007. Luminescence of Bi^{3+} ions in $\text{Y}_3\text{Al}_5\text{O}_{12}:\text{Bi}$ single crystalline films. *Radiat. Meas* 42, 882–886.
- Zorenko, Yu., Mares, J.A., Kucerkova, R., Gorbenko, V., Savchun, V., Voznyak, T., Nikl, M., Beitlerova, A., Jurek, K., 2009. Optical, luminescence and scintillation characteristics of the Bi -doped LuAG and YAG single crystalline films. *J. Phys. D Appl. Phys.* 42, 075501–075507.